Automated Detection of Tonic-Clonic Seizures using 3D Accelerometry and Surface Electromyography in Pediatric Patients

Milica Milošević*, Anouk Van de Vel* Bert Bonroy, Berten Ceulemans, Lieven Lagae, Bart Vanrumste, *Senior Member, IEEE* and Sabine Van Huffel†, *Fellow, IEEE*

***Abstract*—Epileptic seizure detection is traditionally done using video/electroencephalography monitoring, which is not applicable for long-term home monitoring. In recent years, attempts have been made to detect the seizures using other modalities. In this study we investigated the application of four accelerometers (ACM) attached to the limbs and surface electromyography (sEMG) electrodes attached to upper arms for the detection of tonic-clonic seizures. sEMG can identify the tension during the tonic phase of tonic-clonic seizure, while ACM is able to detect rhythmic patterns of the clonic phase of tonic-clonic seizures. Machine learning techniques, including feature selection and least-squares support vector machine classification, were employed for detection of tonic-clonic seizures from ACM and sEMG signals. In addition, the outputs of ACM and sEMG-based classifiers were combined using a late integration approach. The algorithms were evaluated on 1998.3 hours of data recorded nocturnally in 56 patients of which 7 had 22 tonic-clonic seizures. A multimodal approach resulted in a more robust detection of short and non-stereotypical seizures (91%), while the number of false alarms increased significantly compared with the use of single sEMG modality (0.28 to 0.5/12h). This study also showed that the choice of the recording system should be made depending on the prevailing pediatric patient-specific seizure characteristics and non-epileptic behavior.**

***Index Terms*—accelerometry, surface electromyography, seizure detection, pattern recognition, home monitoring**

I. Introduction

EPILEPSY is one of the most common neurological disorders which occurs in 1% of the world population [1]. It is characterized by repetitive epileptic seizures which are the result of excessive brain activity (measured by electroencephalography or EEG) and often accompanied by stereotypical clinical manifestations (recorded by video). Although combined video/EEG monitoring remains the gold standard for epileptic seizure detection, most patients are opposed to wear scalp EEG electrodes for continuous monitoring. Moreover, each time a trained person has to correctly place the EEG electrodes, and during long-term monitoring wearing EEG can become uncomfortable.

Several studies have investigated the detection of different epileptic seizure types using different recording systems. The main focus has been on the detection of (generalized) tonic-clonic (TC) seizures [2], [3], [4], [5], [6], [7], [8], [9], [10]. A TC seizure is a combination of tension resulting in a change of posture followed by a series of jerk-like contractions of agonist and antagonist muscles that regularly occurs at a frequency of 0.2-5 jerks/s [11].

Conradsen et al. (2012) used surface electromyography (sEMG) and an algorithm based on the zero-crossing rate to detect the tonic phase of the TC seizure [8], [9]. On the other hand, other groups used accelerometry (ACM), usually by means of one wrist-worn sensor, to detect the rhythmic pattern of a TC seizure. Applied algorithms ranged from simple thresholding [3], to the use of machine learning techniques [6], [7].

In general, research tends to focus more on the adult population, rather than on children. Only [7] used data recorded solely from children, whereas other publications did not make a distinction between adults and children; however the latter were always underrepresented.

In this paper, we investigated the detection of TC seizures in pediatric patients using ACM and sEMG in both uni- and multi-modal approaches. First ACM and sEMG-based alarm systems were compared, and afterwards these two modalities were merged using late integration. In contrast to the aforementioned publications, which reported seizure duration above 1 minute, some TC seizures within our dataset last only a few seconds. Detection of short events in general leads to the trade-off between detection sensitivity and false detection rate (FDR). In addition, children tend to move more than adults, resulting in a higher number of false alarms compared to the adult population. Taking into consideration the above described challenges, this paper compares machine learning based methodology using ACM and sEMG signals to detect TC seizures in pediatric patients.

Asterisk indicates equal contribution authors. Dagger indicates corresponding author.

M. Milošević, B. Vanrumste and S. Van Huffel† are with the Department of Electrical Engineering (ESAT), STADIUS, KU Leuven and iMinds IT Department, 3000 Leuven, Belgium. e-mail: sabine.vanhuffel@esat.kuleuven.be

A. Van de Vel† and B. Ceulemans are with the Department of Neurology-Paediatric Neurology, University Hospital University of Antwerpen, 2610 Wilrijk, Belgium.

B. Bonroy and B. Vanrumste are with MOBILAB, Thomas More Kempen, 2440 Geel, Belgium.

L. Lagae is with the Department of Child Neurology, University Hospital KU Leuven, 3000 Leuven, Belgium.

B. Ceulemans and L. Lagae are with Rehabilitation Center for Children and Youth Pulderbos, 2242 Pulderbos, Belgium.

B. Vanrumste is with Department of Electrical Engineering (ESAT), Advanced Integrated Sensing (AdvISe), KU Leuven, 2440 Geel, Belgium.

Manuscript received April 0, 2025; revised December 0, 2025.

II. Materials and methods

PATIENT-INDEPENDENT alarm systems were developed using the following steps: data collection, data preprocessing, feature extraction and selection, leave-one-patient-out (LOPO) cross-validation (CV) and training of a LS-SVM (Least-Squares Support Vector Machines) classifier which was tested on the patient left out. Schematic representation of applied methodology is presented on Fig. 1.

A. Data collection

Simultaneous EEG, video and audio, electrocardiography (ECG), sEMG and ACM data were nocturnally recorded in the Rehabilitation Center for Children and Youth in Pulderbos, Belgium. ACM data were collected by four wired three-axial accelerometers attached to the wrists and ankles with elastic bands. The measured range of acceleration was $\pm$3g (g$=9.81$ m/s^2). The range of sEMG signals was $\pm$5mV and the activity of both biceps muscles were registered with this modality. The sampling rate of all signals was 250 Hz.

The study was performed in accordance with the 1964 Declaration of Helsinki and approved by the Medical Ethical Commission of the Antwerp University Hospital, Belgium. Signed informed consent forms from all parents were obtained prior to inclusion in the study. To this end, seven children had in total 31 TC seizures registered both in the ACM and sEMG signals. Seizures were annotated by the trained EEG specialist using the gold standard video/EEG monitoring. Annotations were given as the start and end of clinical manifestation of the seizures. Table I gives an overview of the patients with TC seizures, the number of TC seizures and the number of nights within which these seizure were observed. These data were used to develop the classification algorithms. Apart from TC seizures, within the used database 164 extra seizures longer than 10 seconds were annotated by the EEG expert. The majority of the seizures were frontal lobe seizures with hyperkinetic movements (66), atypical frontal (23), tonic (22) and clonic (18) seizures.

TABLE I
Overview of patients with TC seizures

Patient	♯ TC seizures	♯ nights	Record duration
1	5	2	22:32:24
2	1	5	61:14:12
3	1/9*	2	22:54:48
4	10	1	10:00:13
5	1/2*	7	87:06:44
6	1	2	25:17:52
7	3	1	12:19:29
7 patients	22/31*	20 nights	241:25:43

*Number of TC seizures longer than 10 seconds over total number of TC seizures. For other patients all seizures were longer than 10 seconds.

Apart from seven patients with TC seizures (see Table I), 49 patients with other or no seizures were monitored during 148 nights (around 1757 hours of data). These data were used to better estimate FDR of the developed methodology. The reader can find more clinical information (epileptic syndromes, etiology, seizure types, intellectual and physical development) in the Supplementary materials.

Full recordings were included in the analysis regardless of the record length and quality[1], whether the child was awake or asleep.

B. Data preprocessing

Preprocessing was performed to remove the artifacts and to reduce the data for further processing. ACM data were low-pass filtered with 47 Hz as cut-off frequency in order to remove the power-line and high-frequency interference. After downsampling ACM signals by a factor 2, a high-pass filter of 0.2 Hz cut-off frequency was applied to remove the baseline drifts [12].

A notch filter was used to remove the second harmonic of the power-line interference (100 Hz) from EMG signals (50 Hz was removed within the hardware). In addition, a high-pass filter of 20 Hz cut-off frequency was applied to remove the movement artifacts and baseline noise contamination [13].

The applied filters have linear and/or constant phase responses within the frequency range of interest; hence phase distortion was avoided.

The preprocessed data were divided into 2 second epochs with 75% overlap. An epoch containing more than 50% of seizure activity was labeled as a seizure epoch. Finally, if the standard deviation in each ACM and sEMG channel was respectively lower than 30 mg or 30 μV, the corresponding epoch was removed from further analysis. The thresholds were chosen based on the standard deviation values during clonic phase in ACM signals and tonic phase in sEMG signals. This *activity detection* resulted in a 88.00$\pm$7.64% and 91.46$\pm$9.28% reduction of the initial number of epochs per recording, for ACM and sEMG modalities respectively.

C. Feature extraction

A range of parameters has been used for epileptic seizure classification, from simple time domain, entropy, spectral, wavelet to cross-recurrence plot features. Features extracted from ACM signals were found in the literature [14], [6], [15], [16], [7], [12]. Features used in EEG-based seizure detection [17], [18] and ACM activity recognition [19], [20] were also added to the list. Apart from zero-crossing rate used in [8] for detection of TC seizures using sEMG, we added frequently used features for description of sEMG signals [21], [22]. Starting from $N_f = 149$ ACM and $N_f = 87$ sEMG signal features respectively (which are fully described in the Supplementary materials), a feature selection method based on mutual information was applied, which is described in the next subsection.

Each feature was calculated from each channel ($N_{ch} = 12$ for ACM and $N_{ch} = 2$ for sEMG modality) constituting the one feature matrix $\mathbf{X}^1$ of size $N \times N_{ch}$, hence the total feature matrix with N_f features can be written as follows $\mathbf{X} =$

[1]There were 46 recordings during which one to maximally three of 12 channels were partially or totally not working. This is the consequence of bad connection between the sensor and the cable or the cable and the collection point.

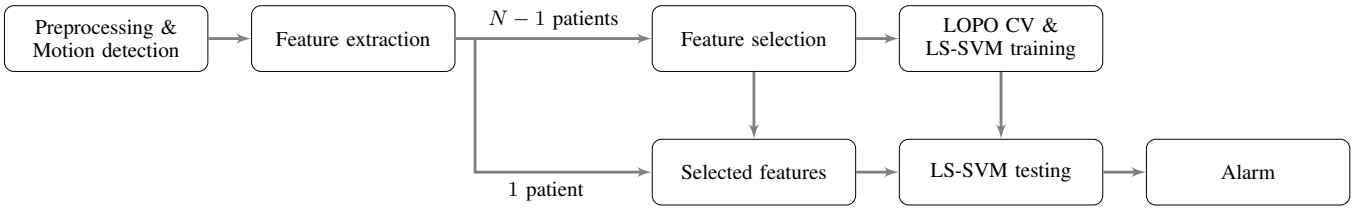


Fig. 1. Schematic overview of the algorithm

$\left[\mathbf{X}^1,\ \mathbf{X}^2,\ \ldots,\ \mathbf{X}^{N_f}\right]$. N is the number of samples/epochs from which features were calculated. The same matrix can be rewritten as follows $\mathbf{X} = [\mathbf{x}_1;\ \mathbf{x}_2;\ \ldots;\ \mathbf{x}_N]$ where $\mathbf{x}_i = [x_{i1},\ x_{i2},\ \ldots,\ x_{id}]$ is the i-th raw vector ($d = N_f \times N_{ch}$). Henceforth, the defined notation is used to describe methods used in this study.

D. Feature selection

The applied filter selection method based on mutual information, called maximal relevance minimal redundancy (mRMR), aims to identify the feature subset within which each selected feature has the highest mutual information with the target class (i.e. label given by the EEG expert) and the minimal mutual information between themselves. Starting from the empty set of chosen features $\mathbf{S} = \emptyset$ and the full set of N_f features $\mathbf{X} = \left[\mathbf{X}^1,\ \ldots,\ \mathbf{X}^{N_f}\right]$, first feature ($j = 1$) was chosen as follows

$$\mathbf{S}^1 = \left\{\mathbf{X}^i \left| \max I\left(\mathbf{X}^i;\mathbf{Y}\right)\right.\right\},\ \mathbf{X}^i \in \mathbf{X} \tag{1}$$

where $\mathbf{Y}$ is the label column multiple to match the size of the feature matrix and I is the mutual information defined as

$$I(\mathbf{u},\mathbf{v}) = \sum_{i,j} p(\mathbf{u}_i,\mathbf{v}_j)\log\frac{p(\mathbf{u}_i,\mathbf{v}_j)}{p(\mathbf{u}_i)\,p(\mathbf{v}_j)} \tag{2}$$

with $p(\mathbf{u})$, $p(\mathbf{v})$ and $p(\mathbf{u},\mathbf{v})$ as probability density functions. Probability density functions were approximated by diffusion-based kernel density estimation, and adaptive kernel density estimation which has proven to outperform existing methods in terms of accuracy and reliability [23].

In case $j \geq 2$, an incremental search is performed using the following condition:

$$\mathbf{S}^j = \left\{\mathbf{X}^l \left| \max_{\mathbf{X}^l \in \mathbf{X}\setminus\mathbf{S}} \left(I\left(\mathbf{X}^l;\mathbf{Y}\right) - \frac{1}{j-1}\sum_{\mathbf{X}^k\in\mathbf{S}} I\left(\mathbf{X}^l;\mathbf{X}^k\right)\right)\right.\right\} \tag{3}$$

where $\mathbf{S}$ is the set of already chosen $j-1$ features. All features for which the mutual information between the feature and target class was higher than the mean mutual information between that feature and the ones that were already chosen, were added to the set of chosen features. Therefore, some redundancy was kept within the feature subset.

E. LS-SVM classification

Support vector machines (SVM) are modern machine learning methods which use kernels to construct a linear classification hyperplane in a higher dimensional space for separation of two different classes data points [24].

If the training data set is denoted as $\{\mathbf{x}_i, y_i\}_{i=1}^N$, with $\mathbf{x}_i \in \Re^d$ being the input vector of features and $y_i \in \{-1,+1\}$ the class labels, SVMs map the d-dimensional input vector $\mathbf{x}$ into the d_h-dimensional space using a (non-)linear function $\varphi(\cdot) : \Re^d \rightarrow \Re^{d_h}$. Then, $\mathbf{w}^T\varphi(\mathbf{x}) + b = 0$ defines the separating hyperplane where $\mathbf{w} \in \Re^d$ is an unknown weighting vector, $b \in \Re$ a constant. Starting from the following formulation

$$y_i\left(\mathbf{w}^T\varphi(\mathbf{x}_i) + b\right) \geq 1, \quad i = 1,\ldots,N, \tag{4}$$

the classifier output is defined as

$$f(\mathbf{x}) = \operatorname{sign}\left(\mathbf{w}^T\varphi(\mathbf{x}) + b\right). \tag{5}$$

In real-life applications, perfect separation is not often possible, thus a certain number of misclassifications around the separation hyperplane should be tolerated. In this case, the resulting optimization problem becomes:

$$\min_{\mathbf{w},\xi,b} J_1(\mathbf{w},\xi) = \frac{1}{2}\mathbf{w}^T\mathbf{w} + C\sum_{i=1}^{N}\xi_i, \tag{6}$$

such that

$$y_i\left(\mathbf{w}^T\varphi(\mathbf{x}_i) + b\right) \geq 1 - \xi_i, \quad \xi_i \geq 1, \quad i = 1,\ldots,N, \tag{7}$$

where C is a positive regularization constant which defines the trade-off between a margin size and misclassification error. Equation 5 can be equivalently written in the dual space using the Lagrange multipliers of support vectors α_i and chosen kernel matrices K:

$$f(\mathbf{x}) = \operatorname{sign}\left(\sum_{i=1}^{\#\mathrm{SV}} \alpha_i y_i K(\mathbf{x},\mathbf{x}_i) + b\right), \tag{8}$$

with $K(\mathbf{x},\mathbf{x}_i) = \varphi(\mathbf{x})^T\varphi(\mathbf{x}_i)$. Many obtained α_i values are equal to zero, meaning that those training points do not contribute to the separation hyperplane. Only the training points close to the boundary are important for its creation ($\alpha_i \neq 0$) and thus they are called support vectors. Therefore, skewed data will not affect the separating hyperplane.

Least-squares support vector machines (LS-SVM) are a modification of the SVM methodology, by introducing a least square loss function and changing the inequalities in equation (4) into equalities [25]. Now instead of solving a quadratic programming problem, we need to solve only the set of linear equations. Therefore, this modification leads to a significant reduction in complexity and computation costs. A LS-SVM classifier optimizes the following problem:

$$\min_{\mathbf{w},e,b} J_2(\mathbf{w},e) = \frac{1}{2}\mathbf{w}^T\mathbf{w} + \gamma\frac{1}{2}\sum_{i=1}^{N} e_i^2, \tag{9}$$

subject to

$$y_i \left(\mathbf{w}^T \varphi\left(\mathbf{x}_i\right) + b\right) = 1 - e_i, \quad i = 1, ..., N, \tag{10}$$

where $e = [e_1,\ e_2,\ ...,\ e_N]^T$ is a vector of error variables. The classifier is again defined by (5) or (8), but now all Lagrange multipliers are different from 0; therefore all training points contribute to the construction of the separating hyperplane. However, the contribution of remote points (even in the large number) is negligible (really low Lagrange multipliers) for the construction of the hyperplane.

We used a RBF (radial basis function) kernel. Kernel and regularization parameters were obtained using LOPO cross-validation. In general, the optimization can be performed using different parameters. Traditionally, it is performed by minimization of the misclassification error, however in case of seizure detection, the data are highly skewed; the seizures are rare events which should be distinguished from all other human motion and normal nocturnal movements. As in [7], the LS-SVM regularization parameters are estimated by maximizing the $F_1 score$ metric, which is the harmonic mean of the sensitivity and positive predictive value of epoch detection. In this case

$$\sum_{i=1}^{N} e_i^2 = 1 - F_1 score = \frac{FP + FN}{2TP + FP + FN}, \tag{11}$$

where TP and TN are the number of correctly identified seizure and non-seizure epochs, respectively. FN represents the number of seizure epochs classified as non-seizure epochs, and FP the number of non-seizure epochs classified as seizure.

Since the tonic and clonic phases are morphologically different both in ACM and sEMG signals, we preselected tonic and clonic segments for sEMG and ACM-based seizure detection algorithms, respectively. The training epochs were randomly chosen from these segments for each modality individually. For each patient maximally 250 seizure and 1000 non-seizure epochs were chosen for training.

We chose to apply leave-one-patient-out (LOPO) testing since the number of seizures per patient was very low, disabling the building of patient-specific models. Moreover, some patients were monitored for only one night also limiting the number of normal movements. In real-life applications, patient-independent algorithms are most practical for seizure detection since the existing detectors built on the previous patients could be applied on a newly arrived epileptic patient.

In case of unimodal seizure detection, only post-processing, explained in the subsection II-F, was performed. Additionally we tested a multimodal approach using late integration by fusing the LS-SVM decisions of ACM (f_{ACM}) and sEMG (f_{sEMG}) modalities. The integration was performed using the inclusive disjunction operation:

$$f_{ACM+sEMG}(\mathbf{x}_i) = f_{ACM}\left(\mathbf{x}_i\right) \vee f_{sEMG}\left(\mathbf{x}_i\right), \tag{12}$$

$i = 1, \ldots, N$. By merging these two decisions the seizure detection probability increased, as shown in subsection III-B.

F. Evaluation metrics

To eliminate possible false detections of short periods, a temporal constraint was applied to the LS-SVM output. The constraint only allowed detection of a seizure after the LS-SVM had classified a number of consecutive epochs containing seizure activity. In general, this post-processing greatly reduces the number of false positives, but also leads to a decreased sensitivity and increased detection latency. The post-processing (number of consecutive epochs needed for positive detection) highly depends on the use of the algorithm. Since ACM is only capable of detecting the clonic phase of the seizure, whereas sEMG the tonic phase, for unimodal TC seizure detection seven consecutive seconds were required to be positively classified by the LS-SVM classifier as a seizure. On the other hand, it was assumed that both phases were detected with the multimodal approach, and therefore the alarm was put on after 10 seconds.

The performances of the developed seizure detectors were characterized in terms of sensitivity, false detection rate per 12 nocturnal hours and detection latency. Sensitivity gives the percentage of test seizures identified by the algorithm. Only TC seizures longer than 10 seconds were taken into consideration for the alarm system, since shorter seizures are not dangerous. False detection rate (FDR) refers to the number of times, over the course of a full night (12 hours), that the detector declared the onset of seizure activity in the absence of an actual TC seizure. In case other seizure types were the cause of an alarm, this alarm was counted as an extra seizure detected. In addition, when nurse/parent's interference led to an alarm, those false alarms were omitted. Examples of these events were the nurse bringing, putting on, removing and testing the system, or handling the child (medication administration, changing the diapers, (un)dressing the child and similar events). At these moments, the real-time alarm system should be turned off beforehand. Latency refers to the delay between expert-marked clinical onset of the seizure and alarm set off by the detection algorithm during the seizure activity.

III. Results

THE previously described methodology was applied to identify TC seizures using ACM or/and sEMG signals. First we checked each modality individually and then late integration was applied to the ACM and sEMG detections. In addition, within each modality, since the number of sensors was large, different sensor combinations were compared regarding the sensitivity and FDR over patients with TC seizures.

A. Unimodal seizure detection

Table II illustrates the classification performances over all seven patients with TC seizures, when different numbers of ACM and sEMG sensors and their combinations within each modality were employed. In addition, the numbers of selected features are added in the table.

When all four ACM sensors were used to build a classifier, 16 of 22 TC seizures were detected, with on average one

TABLE II
ACM/sEMG SENSOR COMBINATION VS SEIZURE DETECTION PERFORMANCE

Sensor(s)*	Sensitivity [%]	FDR/12h	♯ features†
RW	68.18	4.97	3-5
LW	63.64	6.16	4-5
LA	68.18	2.73	6-9
RA	72.73	1.64	3-5
RW+LW	63.64	6.16	4-4
RW+LA	68.18	1.84	3-5
RW+RA	68.18	1.09	3-4
LW+LA	77.27	2.29	4-5
LW+RA	**86.36**	**1.94**	**4-4**
LA+RA	68.18	3.13	3-6
RW+LW+LA	81.82	3.13	4-4
RW+LW+RA	77.27	4.27	4-4
LW+LA+RA	68.18	1.04	4-5
RW+LW+LA+RA	**72.73**	**0.99**	**4-4**
RB	63.64	1.14	1-4
LB	45.45	2.09	1-3
RB+LB	**81.82**	**0.60**	**1-2**

*RW = right wrist ACM, LW = left wrist ACM, LA = left ankle ACM, RA = right ankle ACM, RB = right biceps sEMG, LB = left biceps sEMG;
†Feature selection was performed for each patient by excluding that particular patient. Therefore the number of selected features and selected features were often different among the patients.

false alarm per night. Combining three ACM sensors if two of which were wrist sensors increased the sensitivity, however the false detection rate also significantly increased. Left wrist and right ankle ACM positions resulted in the identification of 19 TC seizures (the highest sensitivity), but also false detection rate increased by two compared with the use of the complete ACM-based measurement system. Finally, using only one wrist ACM sensor caused too many false positives to be used for an alarm system.

In general, the following features were found to be relevant for ACM-based distinction of TC seizures from other movements: number of local maxima in the signal [17], Shannon entropy of diagonal line lengths in cross-recurrence plot [7], [26], frequency of the first local peak in the spectrum and power within scale range 5-11 (corresponding pseudo-frequency range 9-22.5 Hz) from continuous wavelet transform obtained using Morlet mother wavelet [14]. There were slight differences when different ACM sensors were used, but in case the highest sensitivity was reached (two ACM sensors) and in case the lowest FDR was accomplished (all ACM sensors), all aforementioned features were chosen for all patients (in a LOPO procedure).

Table II suggests that the detection of TC seizures with only one sEMG sensor was not reliable both regarding sensitivity and false detection rate. Combining right and left biceps sEMG data, 18 TC seizures were detected with 3 false alarms within 5 nights, outperforming ACM-based TC seizure detection. The most relevant feature for detection of TC seizures was Wilson amplitude [21], then the zero-crossing rate of the second derivative and the number of local maxima [17] in sEMG signals. A table with all feature selection results is presented in the Supplementary materials.

Since the seizure detection and FDR vary significantly over the patients, the results for each patient with TC seizure(s) and each modality are presented in Table III.

Sensitivity per patient was either 0 or close to 100%, meaning that the seizure detection depended on the seizure characteristics and used modalities. For instance, patient 5 had only one seizure, and although the seizure was 21 seconds long, it had a clonic phase shorter than the algorithm's requirements for ACM-based detection (around 6 seconds and only three jerks). The opposite was true for the TC seizure of patient 2, with a short tonic phase (around 4 seconds). Patient 7 experienced TC seizures of around 1 minute, however due to obstruction of the limbs the clonic pattern was disrupted and discontinuous (child was lying in supine position and was trying to get up). The one seizure of patient 2 was never detected, probably due to the low frequency of the jerks.

Values of FDR were influenced by patient-specific behavior. Children with epilepsy tend to have a specific pattern of behavior, which was sometimes similar to the seizure patterns. For instance, patients 2, 5 and 6 before falling asleep, frequently started clapping, they uncontrollably rubbed or shacked the hands. Patient 4 in early morning hours started trembling, similarly to the clonic pattern of TC seizures. Previously mentioned behavior most often resulted in false alarms in ACM-based seizure detectors. On the other hand, sEMG was sensitive to stretching and tension-line turning which were typical for patient 3.

As shown in Table III, detection latency was on average lower for sEMG-based seizure detection compared with the ACM system. This result was logical, since the clonic phase detected by ACM is preceded by the tonic phase detected by sEMG modality. However, the latency differences were not large, since mainly all TC seizures were short seizures.

We repeated the whole methodology scheme (see Fig. 1) using seven patients with TC seizures for the feature selection and LS-SVM training. The obtained algorithm was tested on 49 patients who did not experience TC seizures. The number of test nights per patient ranged from 1 to 22 nights. The same subsets of features were obtained as in LOPO procedures for both modalities. Fig. 2 and 3 display the histograms of FDR/12h for these patients using ACM- and sEMG-based seizure detection, respectively.

The results strongly suggest that sEMG is less sensitive to false alarms (overall 46 false alarms in 1998.3 hours). In contrast, dispersion of the FDR histogram is increased for ACM-based seizure detection, whether four or two ACM sensors were used. For the majority of the patients the FDR was 0, whereas for some patients due to the high FDR other solutions have to be found. Individual FDR values per patient can be found in the Supplementary materials.

B. Multimodal seizure detection

We chose to perform the late integration of the outputs of two ACM and two sEMG sensors, since the performance between two and four ACM sensors was not significantly different whereas the number of sensors makes a big difference.

TABLE III
UNIMODAL CLASSIFICATION RESULTS

	4 ACM sensors			2 ACM sensors			2 sEMG sensors		
Patient	Sensitivity [%]	Latency [s]	FDR/12h	Sensitivity [%]	Latency [s]	FDR/12h	Sensitivity [%]	Latency [s]	FDR/h
1	100	13.2	0.00	100	13.4	0.00	80	12.2	0.00
2	0	-	1.96	0	-	5.49	0	-	0.00
3	100	7.3	0.00	100	7.3	0.00	0	-	5.76
4	90	20.5	3.60	100	20.5	0.00	100	14	1.20
5	0	-	0.55	0	-	0.96	100	7.3	0.00
6	100	15	1.42	100	15	1.90	100	10.5	0.00
7	0	-	0.00	66.67	22.8	0.00	66.67	7.3	0.00
Total*	72.73	15.55	0.99	86.36	19.4	1.94	81.82	10.5	0.60

*Overall sensitivity is calculated as total number of detected TC seizures over the total number of TC seizures. Latency value is median latency over all detected seizures and FDR is calculated only for patients with TC seizures.

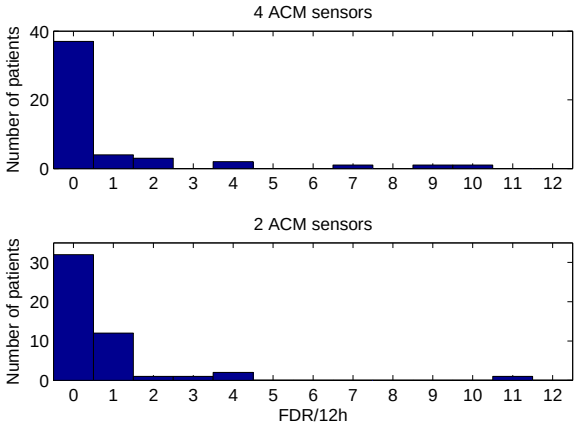


Fig. 2. Histogram of FDR/12h for patients without TC seizures when all four ACM sensors are used, and when only left wrist and right ankle ACM sensors are used.

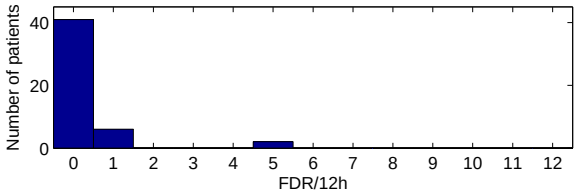


Fig. 3. Histogram of FDR/12h for patients without TC seizures when two sEMG sensors attached to the child's biceps are used.

More weight was given to sensitivity over FDR. 20 of 22 TC seizures were correctly identified and there were nine false alarms within 20 nights of patients with TC seizures. Table IV displays algorithm performances per patient. In addition, Fig. 4 shows the histogram of FDR/12h over the patients without TC seizures. Including sEMG, one extra seizure was correctly identified, while the number of false alarms dropped from 162 to 83. Still this was twice as much the number of false alarms using only the sEMG modality (in total 46 false alarms).

IV. DISCUSSION

IN this study, we investigated the use of sEMG and ACM sensors for the detection of TC seizures in pediatric patients. Since the number of sensors was high, an analysis was performed to assess the relevance of the number and position of sensors. Concerning the ACM modality, a two sensor set-up was found to not significantly degrade the algorithm performance compared with the full setup. Left wrist (i.e. generally non-dominate hand) and right ankle were identified as the optimal positions for ACM sensors. Concerning the sEMG sensors, it was not possible to reduce the number of sensors to only one. One possible explanation would be that the biceps muscles are not the best positions for TC seizure registration and detection [8].

The 0% sensitivities for patients 2, 3, 5 and 7 (either with ACM only, sEMG only or a combination of both) could be partially explained by their respective hypotonia, left hemiplegia, diplegia and mostly right sided spastic quadriplegia. Neurological background information (see Supplementary

TABLE IV
MULTIMODAL (AMC AND SEMG) CLASSIFICATION RESULTS

Patient	Sensitivity [%]	Latency [s]	FDR/12h
1	100	8.7	0.00
2	0	-	1.18
3	0	-	0.00
4	100	14	0.00
5	100	7.3	0.28
6	100	10.5	0.47
7	100	15	0.00
Total*	90.91	10.5	0.45

*Overall sensitivity is calculated as total number of detected TC seizures over the total number of TC seizures. Latency value is median latency over all detected seizures and FDR is calculated only for patients with TC seizures.

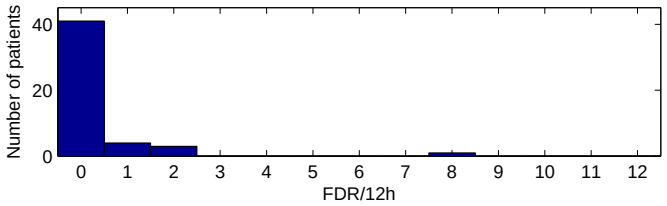


Fig. 4. Histogram of FDR/12h for patients without TC seizures when left wrist and right ankle ACM sensors are combined with two sEMG sensors.

TABLE V
COMPARISON OF STUDIES INVOLVING ACM AND SEMG-BASED TC SEIZURE DETECTION METHODS

Publication	Kramer (2011) [5]	Poh (2013) [7]	Beniczky (2013) [10]	Milošević (2015)	Conradsen (2012) [8]	Conradsen (2012) [9]	Milošević (2015)	Milošević (2015)
Sensor(s)	1 ACM	1 ACM + EDA*	1 ACM	2 ACM	1 sEMG	1 sEMG	2 sEMG	2 ACM + 2 sEMG
Population [y]	-	9-14.2	6-68	0.7-18.5	11-62	34-48	0.7-18.5	0.7-18.5
# patients†	15/31	7/80	20/73	7/56	11/60	2/4	7/56	7/56
# seizures	22	16	39	22	22	7	22	22
Seizure types‡	T, C, TC	GTC	GTC	TC	GTC	GTC	TC	TC
Seizure duration	$\geq$20 s	$\geq$60 s	-	$\geq$10 s	-	$\geq$50 s	$\geq$10 s	$\geq$10 s
Record duration	1692h	4213h	4878h	1998h	776h	298h	1998h	1998h
Sensitivity	91% (20/22)	94% (15/16)	90% (35/39)	86% (19/22)	100% (22/22)	57% (4/7)	82% (18/22)	91% (20/22)
FDR♮	0.11/24h	0.74/24h	0.2/24h	0.97/12h	0.04/24h	0.07/24h	0.28/12h	0.5/12h
Median latency	17 s	31.4 s	55 s	19.4 s	13.7 s	24.5 s	10.5 s	10.5 s

*EDA = ElectroDermal Activity;
†Number of patients with seizures over total number of patients;
‡TC = tonic-clonic, GTC = generalized tonic-clonic, T = tonic, C = clonic seizures;
♮While other studies monitored the patients day and night, we did it only during the night, hence different FDR measurement units

materials) could br partially linked with obtained FDR values. For instance, the syndrome with unvoluntary movements of patient 2 helped to understand the false detection rate of up to five per night in this patient (2 ACMs), however we do not have a uniform explanation for the up to six false detections per night in patient 3 who executed many stretches and turns (2 sEMG sensors), and up to four in patient 4 who trembled for long periods of time (4 ACMs). These two patients have an intellectual disability but no specific motor development problem.

Based on the available data, sEMG was significantly less sensitive to false alarms, while only one TC seizure was not identified by sEMG when compared with the ACM modality. Over all patients, sEMG experienced 46, whereas 152 and 162 false alarms were observed within 1998.3 hours using four and two ACM sensors, respectively. Although, the total number of false alarms obtained from ACM signals were 3.3 and 3.5 times higher using four and two ACM sensors, 40 and 45% of these events were "events of interest". Most of these events were of one particular child hitting the pillow with the head (typical strange behavior of this child), pulling the EEG electrodes, falling off the bed, trying to remove the sensors, and similar dangerous situations, when assistance was needed. On the other hand, sEMG was insensitive to these kinds of events, except to pulling off the EEG electrodes. Applying late integration on two ACM and sEMG sensors classification decisions, not only the sensitivity increased, but also the FDR decreased. Out of 83 false alarms, we observed 43 events in which assistance was needed.

As seen in Table II, depending on which sensor combination was employed, the number and features chosen in the LOPO testing approach often differed. When the complete set or two ACM sensors (left wrist and right ankle) were employed, the number and chosen features did not depend on the patient who was excluded from the data. This is highly practical for the development of a generic algorithm for detection of TC seizures. It also suggests that chosen features have universal relevance for TC seizure detection using ACM signals. However, this was not the case when two sEMG signals were used to detect TC seizures. The Wilson amplitude appeared in all feature sets. The second feature was the zero-crossing rate of the second derivative which appeared four times, whereas the number of local maxima appeared only in one feature set. It would be interesting to investigate if the fixed feature set (use always these three features or only the Wilson amplitude) for all patients significantly influences the detection performance.

In general, features selected for sEMG seizure detection (Wilson amplitude, zero-crossing rate and number of local maxima) are all clinical features. However, in case of ACM seizure detection, apart from local maxima in the signal which can be considered a clinical feature, other features identified by the feature section algorithm are not used by an expert to visually score the data. These features are Shannon entropy of diagonal line lengths in cross-recurrence plot, frequency of the first local peak in the spectrum and power within scale range 5-11 (corresponding pseudo-frequency range 9-22.5 Hz) from continuous wavelet transform obtained using Morlet mother wavelet.

Using the developed TC detection algorithms, other seizure types were also detected. Using sEMG, 31 extra seizures were identified; predominantly tonic seizures (14), frontal lobe seizures with hyperkinetic movements (10) and three TC seizures shorter than 10 seconds. The same number of extra seizures was registered using two ACM sensors; among them there were 12 frontal lobe seizures with hyperkinetic movements, four clonic, four tonic and two TC seizures shorter than 10 seconds. Even though the methods were not trained to detect other types of epileptic convulsions, on average 18% of them were detected. We expected to detect more clonic seizures (at least using ACM modality), since the clonic phase and clonic seizures are similar. In general, the clonic phase of TC seizures was intensive with high-frequency jerk-like movements, whereas clonic seizures encountered in our database had a different movement frequency making it difficult to detect them with the features optimized for TC seizures with high frequency jerk-like movements. In case of

tonic seizures, a large number of tonic seizures were correctly identified by the sEMG-based TC seizure detector even though Conradsen et al. [27] found that sustained muscle activation during the tonic phase of TC seizure is different from that during tonic seizures. The tonic phase of TC seizures is characterized by an increased amplitude whereas tonic seizures are produced by a significant increase in the frequency of the signal.

Finally, we compared the obtained results with publications reporting on TC seizure detection (alarm system) using one or more body-attached sensors (ACM or sEMG) that used real-life data and did not preselect the data. Table V contains the study information regarding the listed publications. Sensitivity obtained within this study using an unimodal approach was a bit lower, whereas our multimodal approach had comparable sensitivity in the range of detection rates reported by other publications [5], [7], [10], [8]. As indicated in Table V, the FDRs for both approaches were much higher than in other studies, even though our recordings were performed only nocturnally whereas others did it day and night. This difference in set-up makes the comparison difficult. However, FDR of 0.28/12h obtained using two sEMG sensors is comparable to 0.74/24h obtained using a biosensor based on ACM and electrodermal activity [7]. In both cases, pediatric patients were monitored, which generally tend to move more than adults. This could explain the higher FDRs. Median detection latency on average was higher using ACM sensors [5], [7], [10] compared with the sEMG [8], [9]. Using ACM sensors, we obtained a detection latency either comparable or much lower than other studies, whereas using sEMG sensors the latency was always lower. The seizures recorded in Pulderbos Rehabilitation center were in general short seizures which led to building the alarm system with a short detection latency. Increasing the latency, would decrease the FDR. However, in that case, only the longest seizures would be detected by the alarm system.

In the future, we plan to investigate the influence of a fixed feature set for all patients calculated from sEMG signals on the detection performance, compared with the features obtained within the LOPO procedure used in this study. In addition, the measurement of other body signals (such as ECG) individually or in combination with other modalities will be studied in order to improve the sensitivity for the patients whose seizures were difficult to detect with patient-independent algorithms based on ACM or sEMG signals.

V. Conclusion

WITHIN this study, the detection of tonic-clonic epileptic convulsions was accomplished with the use of 3D accelerometry and surface electromyography. It was shown that the use of two ACM sensors (non-dominant wrist and one leg) gave comparable performances compared to the full set of four ACM sensors attached to the wrists and ankles. Over all patients, sEMG showed lower susceptibility for false alarms compared with the ACM signals. However, high inter-patient variability was observed regarding FDR values, with a majority of patients experiencing no or a really small number of false alarms, indicating the need for a patient-specific measurement system for detection of epileptic convulsions based on prior knowledge on patient's seizure characteristic and his/her typical non-epileptic behavior.

Acknowledgment

Research supported by Research Council KUL: CoE PFV/10/002 (OPTEC), several PhD/Postdoc grants; FWO projects: G.0427.10N (Integrated EEG-fMRI), G.0108.11 (Compressed Sensing), G.0869.12N (Tumor imaging), G.0A5513N (Deep brain stimulation), FWO-PhD/Postdoc grants; IWT projects: TBM 080658-MRI (EEG-fMRI), TBM 110697-NeoGuard, IWT-PhD/Postdoc grants; iMinds Medical Information Technologies SBO 2015, ICON: NXT_Sleep; Flanders Care: Demonstratieproject Tele-Rehab III (2012-2014); Belgian Federal Science Policy Office: IUAP P7/19/ (DYSCO, 'Dynamical systems, control and optimization', 2012-2017); Belgian Foreign Affairs-Development Cooperation: VLIR UOS programs; EU: The research leading to these results has received funding from the European Research Council under the European Union's Seventh Framework Programme (FP7/2007-2013) / ERC Advanced Grant: BIOTENSORS (n^o 339804); This paper reflects only the authors' views and the Union is not liable for any use that may be made of the contained information. RECAP 209G within INTERREG IVB NWE programme, EU MC ITN TRANSACT 2012 (n^o 316679), ERASMUS EQR: Community service engineer (n^o 539642-LLP-1-2013)

References

[1] A. Van de Vel, K. Cuppens, B. Bonroy, M. Milosevic, K. Jansen, S. Van Huffel, B. Vanrumste, L. Lagae, and B. Ceulemans, "Non-EEG seizure-detection systems and potential SUDEP prevention: State of the art," *Seizure*, vol. 22, pp. 345–355, 2013.

[2] C. Carlson, V. Arnedo, M. Cahill, and O. Devinsky, "Detecting nocturnal convulsions: efficacy of the MP5 monitor," *Seizure*, vol. 18, no. 3, pp. 225–227, 2009.

[3] E. Schulc, I. Unterberger, S. Saboor, J. Hilbe, M. Ertl, E. Ammenwerth, E. Trinka, and C. Them, "Measurement and quantification of generalized tonic–clonic seizures in epilepsy patients by means of accelerometry – An explorative study," *Epilepsy Research*, vol. 95, no. 1, pp. 173–183, 2011.

[4] J. Lockman, R. Fisher, and D. Olson, "Detection of seizure-like movements using a wrist accelerometer," *Epilepsy & Behavior*, vol. 20, no. 4, pp. 638–641, 2011.

[5] U. Kramer, S. Kipervasser, A. Shlitner, and R. Kuzniecky, "A novel portable seizure detection alarm system: preliminary results," *Journal of Clinical Neurophysiology*, vol. 28, no. 1, pp. 36–38, 2011.

[6] I. Conradsen, S. Beniczky, P. Wolf, T. W. Kjaer, T. Sams, and H. B. Sorensen, "Automatic multi-modal intelligent seizure acquisition (MISA): system for detection of motor seizures from electromyographic data and motion data," *Computer Methods and Programs in Biomedicine*, vol. 107, no. 2, pp. 97–110, 2012.

[7] M.-Z. Poh, T. Loddenkemper, C. Reinsberger, N. C. Swenson, S. Goyal, M. C. Sabtala, J. R. Madsen, and R. W. Picard, "Convulsive seizure detection using a wrist–worn electrodermal activity and accelerometry biosensor," *Epilepsia*, vol. 53, no. 5, pp. e93–e97, 2012.

[8] I. Conradsen, S. Beniczky, K. Hoppe, P. Wolf, and H. B. Sorensen, "Automated algorithm for generalized tonic–clonic epileptic seizure onset detection based on sEMG zero-crossing rate," *IEEE Transactions on Biomedical Engineering*, vol. 59, no. 2, pp. 579–585, 2012.

[9] I. Conradsen, S. Beniczky, P. Wolf, P. Jennum, and H. B. Sorensen, "Evaluation of novel algorithm embedded in a wearable sEMG device for seizure detection," in *Proceedings of the Annual International Conference of the IEEE Engineering in Medicine and Biology Society (EMBC)*. IEEE, 2012, pp. 2048–2051.

[10] S. Beniczky, T. Polster, T. W. Kjaer, and H. Hjalgrim, "Detection of generalized tonic–clonic seizures by a wireless wrist accelerometer: A prospective, multicenter study," *Epilepsia*, vol. 54, no. 4, pp. 58–61, 2013.
[11] H. Lüders, J. Acharya, C. Baumgartner, S. Benbadis, A. Bleasel, R. Burgess, D. Dinner, A. Ebner, N. Foldvary, E. Geller *et al.*, "Semiological seizure classification*," *Epilepsia*, vol. 39, no. 9, pp. 1006–1013, 1998.
[12] K. Cuppens, P. Karsmakers, A. Van de Vel, B. Bonroy, M. Milosevic, S. Luca, T. Croonenborghs, B. Ceulemans, L. Lagae, S. Van Huffel *et al.*, "Accelerometry-based home monitoring for detection of nocturnal hypermotor seizures based on novelty detection." *IEEE Journal of Biomedical and Health Informatics*, vol. 18, no. 3, pp. 1026–1033, 2014.
[13] C. J. De Luca, L. Donald Gilmore, M. Kuznetsov, and S. H. Roy, "Filtering the surface EMG signal: Movement artifact and baseline noise contamination," *Journal of Biomechanics*, vol. 43, no. 8, pp. 1573–1579, 2010.
[14] G. Becq, S. Bonnet, L. Minotti, M. Antonakios, R. Guillemaud, and P. Kahane, "Classification of epileptic motor manifestations using inertial and magnetic sensors," *Computers in Biology and Medicine*, vol. 41, no. 1, pp. 46–55, 2011.
[15] T. Nijsen, R. Aarts, J. Arends, and P. Cluitmans, "Automated detection of tonic seizures using 3–D accelerometry," in *Proceedings of the 4th European Conference of the International Federation for Medical and Biological Engineering*. Springer, 2009, pp. 188–191.
[16] T. Nijsen, R. Aarts, P. Cluitmans, and P. Griep, "Time–frequency analysis of accelerometry data for detection of myoclonic seizures," *IEEE Transactions on Information Technology in Biomedicine*, vol. 14, no. 5, pp. 1197–1203, 2010.
[17] A. Temko, E. Thomas, W. Marnane, G. Lightbody, and G. Boylan, "EEG-based neonatal seizure detection with support vector machines," *Clinical Neurophysiology*, vol. 122, no. 3, pp. 464–473, 2011.
[18] L. Logesparan, A. J. Casson, and E. Rodriguez-Villegas, "Optimal features for online seizure detection," *Medical & Biological Engineering & Computing*, vol. 50, no. 7, pp. 659–669, 2012.
[19] D. Karantonis, M. Narayanan, M. Mathie, N. Lovell, and B. Celler, "Implementation of a real–time human movement classifier using a triaxial accelerometer for ambulatory monitoring," *IEEE Transactions on Information Technology in Biomedicine*, vol. 10, no. 1, pp. 156–167, 2006.
[20] S. Preece, J. Goulermas, L. Kenney, and D. Howard, "A comparison of feature extraction methods for the classification of dynamic activities from accelerometer data," *IEEE Transactions on Biomedical Engineering*, vol. 56, no. 3, pp. 871–879, 2009.
[21] I. Mesa, A. Rubio, J. Diaz, J. Legarda, and B. Sedano, "Reducing the number of channels and signal-features for an accurate classification in an emg pattern recognition task." in *Proceedings of the International Conference on Bio-inspired Systems and Signal Processing (BIOSIGNALS)*. SciTePress, 2012, pp. 38–48.
[22] J. Shi, Y. Cai, J. Zhu, J. Zhong, and F. Wang, "sEMG-based hand motion recognition using cumulative residual entropy and extreme learning machine," *Medical & Biological Engineering & Computing*, vol. 51, no. 4, pp. 417–427, 2013.
[23] Z. Botev, J. Grotowski, D. Kroese *et al.*, "Kernel density estimation via diffusion," *The Annals of Statistics*, vol. 38, no. 5, pp. 2916–2957, 2010.
[24] V. Vapnik, *The nature of statistical learning theory*. Springer, 1999.
[25] J. A. K. Suykens, T. Van Gestel, J. De Brabanter, B. De Moor, and J. Vandewalle, *Least squares support vector machines*. World Scientific Pub. Co., Singapore, 2002.
[26] N. Marwan, M. Carmen Romano, M. Thiel, and J. Kurths, "Recurrence plots for the analysis of complex systems," *Physics Reports*, vol. 438, no. 5, pp. 237–329, 2007.
[27] I. Conradsen, P. Wolf, T. Sams, H. B. Sorensen, and S. Beniczky, "Patterns of muscle activation during generalized tonic and tonic–clonic epileptic seizures," *Epilepsia*, vol. 52, no. 11, pp. 2125–2132, 2011.